# QSAR MODELING FOR ANTIOXIDANT ACTIVITY OF NOVEL N³ SUBSTITUTED 5,7-DIMETHYL-3*H*-THIAZOLO[4,5-*b*]PYRIDIN-2-ONES

**O. Klenina[1*], T. Chaban[1], B. Zimenkovsky[2], S. Harkov[3], V. Ogurtsov[1], I. Chaban[4], I. Myrko[1]**

[1]Department of General, Bioinorganic, Physical and Colloidal Chemistry
Danylo Halytsky Lviv National Medical University, Ukraine
Pekarska 69, Lviv, 79010, Ukraine
[2]Department of Pharmaceutical, Organic and Bioorganic Chemistry
Danylo Halytsky Lviv National Medical University, Ukraine
Pekarska 69, Lviv, 79010, Ukraine
[3]Department of Pharmacy
Medical College of Burgas University "Prof. Dr. Asen Zlatarov"
St. Stambolov 69 Blv., Burgas, 8000, Bulgaria
[4]Department of Pharmaceutical Chemistry FPGE
Danylo Halytsky Lviv National Medical University, Ukraine
Pekarska 69, Lviv, 79010, Ukraine

## Abstract

The intensive researches have been focused on the novel five-membered heterocyclic systems synthesis in nowadays organic, pharmaceutical and medical chemistry as the promising drug candidates whose quotient among the existing drugs is significant. Thiazolopyridines have the wide range of biological actions on account of their iso-steric to pyrine and pyrimidine bases structure. Therefore functional modification of the mentioned heterocyclic system and its novel analogs biological activity evaluation is actually purposeful.

A series of N³ substituted 5,7-dimethyl-6-phenylazo-3*H*-thiazolo[4,5-*b*]pyridine-2-one derivatives were evaluated *in vitro* for their free radicals scavenging effect which allowed to identify three lead compounds possessing considerable antioxidant action.

QSAR studies for the compounds were performed incorporating 1*D*, 2*D*, 3*D* and quantum-chemical descriptors into respective models as their computation involved integration of the relevant molecular information regarding molecular composition, atom-centered fragments, size, shape, symmetry, atoms and distances distribution in the geometrical representation of the molecules. It had been demonstrated statistically that achieved QSAR models (possessed considerable $R^2$, $Q^2$, $F$ values) could be used for identifying novel antioxidant agents based on the same congeneric series which may be considered as the systematic approach for rational design and virtual screening of novel 3*H*-thiazolo[4,5-*b*]pyridine-2-one derivatives as drug candidates.

**Graphical abstract**

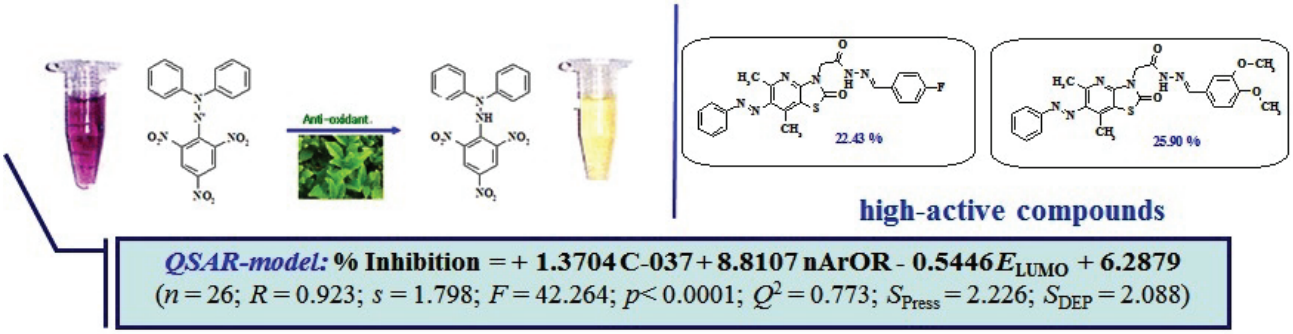


**Keywords:** thiazolo[4,5-*b*]pyridines, DPPH, antioxidant activity, QSAR-analysis, molecular descriptors

## Introduction

The challenge of equally importance in modern medicine and pharmacy is the chemical regulation of numerous pathological conditions caused by the development of oxidative stress in a living organism, and researching the biochemical mechanisms inhibiting free radical processes. The available antioxidants used for the oxidative stress regulation are natural compounds or synthetic drugs. However, according to clinical and experimental data, these drugs exhibit a number of side effects. Increased interest in the establishment of preventive and therapeutic synthetic origin antioxidants determines the relevance of developing and improving methods for antioxidant activity evaluation.

Therefore, the discovery of antioxidant agents is a recent problem that requires new methodological approaches development for the synthesis of novel compounds and their pharmacological activity screening, while it is also the society relevant task of life sciences, including pharmaceutical and medical chemistry.

The vast majority of modern marketed drugs belong to heterocyclic compounds while thiazolidine derivatives represent one of the most important classes among them. Thiazolidine core is a powerful and effective pattern for rational design of "drug-like" molecules as prototypes of innovative therapeutics, thus condensed heterocyclic systems for which 4-thiazolidones are synthetic precursors will produce structural leads allowing further derivatization with retaining drug-like characteristics. 4-Thiazolidine moiety heterocycles and their pyridine fused analogs have acquired much importance because of their diverse pharmaceutical applications. For example, some of their derivatives are known as useful antimicrobial agents effective against a variety of human and veterinary pathogens [1]. Thiazolo[4,5-*b*]pyridines were also shown to possess strong inhibitory actions for A *β*42 fibrillization at the micromolar level for Alzheimer's disease treatment [2]. The significant antiexcudative, antimicrobial and antioxidant effects of some thiazolo[4,5-*b*]pyridine derivatives had been also reported [3-8]. Some of their analogues were recognized as H3 receptor antagonists [9, 10] or act as antagonists of metabotropic glutamate receptors 5 (mGluR5) [11], other ones were revealed as potent inhibitors with respect to the receptors of the epidermal growth factor [12]. Some of them are able to activate the GK enzyme *in vitro* and significantly reduce glucose level [13] and may be utilized as analytical reagents [14].

A considerable amount of effort has been expended over the recent decade to increase

the success rate of the drug discovery process. Modern strategies application for potential therapeutics development are aimed on the potent lead compounds identification for a pre-selected protein target from the virtual library of drug-like chemicals using receptor-based and ligand-based virtual screening techniques. The most potent compounds are selected for chemical optimization towards the specific molecular target. There are essentially two ways for the discovery of new drugs: rational design and massive screening. Computer-aided drug design methods have been very useful in order to perform rational analysis of biological activities [15]. The quantitative structure-activity relationship (QSAR) studies provide remarkable information on the structural feature of novel drug candidates been one of the techniques used to investigate the correlation between biological activities and the physicochemical properties of the set of molecules. This ranks the feature of the compounds that needed to enhance the desirable biological effect.

The true utility of thiazolidine core is the ability to generate one virtual combinatorial library based upon one score scaffold and screened it against a variety of different receptors yielding a series of active compounds. Therefore functional modification of the mentioned heterocyclic system and its novel analogs biological activity evaluation is actually purposeful.

**Experimental Part**

During the recent years the efficient synthetic approach for 3*H*-thiazolo[4,5-*b*]pyridine-2-one system construction had been developed as the protocol based on [3+3] cyclocondensation of 4-iminothiazolidine-2-one on account of its N,C-binucleophylic properties with dielectrophylic reagents like acetylacetone [16]. 6-Phenylazo-5,7-dimethyl-3*H*-thiazolo[4,5-*b*]pyridine-2-one was obtained under the reaction of 4-iminothiazolidine-2-one with arylazoacetone.

Core thiazolo[4,5-*b*]pyridine scaffold had been extensively studied as electrophilic reagent implemented on account of NH-group hydrogen atom. This offered its functionalization featuring novel $N^3$-substituted 5,7-dimethyl-6-phenylazo-3*H*-thiazolo[4,5-*b*]pyridine-2-one derivatives. Thus NH-center made it possible to involve its potassium salt into N-alkylation reaction with the appropriate alkyl halides which allowed to obtain 3-alkyl 5,7-dimethyl-3*H*-thiazolo[4,5-*b*]pyridine-2-one derivatives. In order to further explore the synthetic potential of 5,7-dimethyl-3*H*-thiazolo[4,5-*b*]pyridine-2-one potassium salt aimed on its structural functionalization in $N^3$ position 3-carboxymethyl-substituted 5,7-dimethyl-6-phenylazo-3*H*-thiazolo[4,5-*b*]pyridine-2-one amides and (5,7-dimethyl-2-oxo-6-phenylazo-3*H*-thiazolo[4,5-*b*]pyridine-3-yl)-acetic acid ethyl ester were synthesized. The latest was utilized as a convenient precursor for (5,7-dimethyl-2-oxo-6-phenylazo-thiazolo[4,5-*b*]pyridine-3-yl)-acetic acid hydrazide obtaining as a key step for its hydrazide center further incorporating into chemical transformations. The synthetic potential of hydrazide group in $N^3$ position of (5,7-dimethyl-2-oxo-6-phenylazo-thiazolo[4,5-*b*]pyridine-3-yl)-acetic acid hydrazide was demonstrated as its utility with aromatic aldehydes.

In our previous papers [3, 6] we reported synthesis of 29 novel $N^3$ substituted 5,7-dimethyl-3*H*-thiazolo[4,5-*b*]pyridine-2-one derivatives using the developed synthetic protocols.

*In Vitro Antioxidant Assay*

The antioxidant activity evaluation of the novel compounds was fulfilled with the use of spectrophotometric assays based on the potential antioxidants free radical scavenging potency evaluation. DPPH assay was utilized for antioxidant activity determination [17, 18] with minor modifications.

The solution of DPPH in ethanol with the concentration of 150 μmoles/L (4 mL) was mixed with the compound or control solution in ethanol its concentration been 250 μmoles/L (0.2 mL). The reaction mixture was vortex mixed thoroughly and incubated at room temperature in

the dark for 60 min. Simultaneously, a control was prepared as ascorbic acid solution in ethanol (0.2 mL) mixed with of DPPH solution in ethanol (4 mL) without sample fraction. Reduction in the absorbance of the mixture was measured using ethanol as blank. Ascorbic acid was used as a standard. Also the absorbance of DPPH solution was measured. Percentage of free-radical-scavenging activity was expressed as percent inhibition and it was calculated using the following formula:

$$\% \text{ Inhibition} = \frac{A_{DPPH} - A_c}{A_{DPPH}} \cdot 100\,\%$$

where $A_{DPPH}$ is the absorbance of DPPH free radicals solution, $A_c$ is the absorbance of a sample.

Each experiment was performed in triplicate and average values were recorded. Results are expressed as the means ± S.D.

*Chemical structures optimization and calculation of molecular descriptors*

The series of 29 novel previously synthesized $N^3$ substituted 3*H*-thiazolo[4,5-*b*]pyridine-2-one derivatives [3, 6] possessed free radical scavenging effect were considered for QSAR study. 2*D* structures of all molecules were drawn with ACD/ChemSketch chemical formulas redactor. Later on they were converted to 3*D* structures using Hyper-Chem 7.5 software [19]. The license on HyperChem 7.5 software is available for Danylo Halytsky Lviv National Medical University, Lviv, Ukraine.The model built and the molecular mechanics energy minimization of all compounds were carried out by using the MM+ force field, and repeated minimization was performed using semi-empirical AM1 quantum-chemical method until the root-mean-square (rms) deviation of 0.01 kcal/mol would be achieved. Conformations of compounds were optimized through semi-empirical AM1 method with the global minimum selection among all energy-minimal conformers. 3*D* globally minimized structures as hin Hyper-Chem output were converted into smi format, SD file was prepared with E-BABEL on-line version [20].

SD file prepared with 3*D* structures of the compounds was utilized as inputs for E-DRAGON software [20]. The software was used for calculating 20 subsets of molecular descriptors. The structural parameters calculated after discarding the constant and near constant values (over 1666 descriptors) were saved and further analyzed.

*Descriptors selection strategy and predictive QSAR models generation*

Multiple linear regression (MLR) analysis implemented into BuildQSAR software application [21] was used to perform the QSAR studies. The statistical processing of the QSAR models obtaining was carried out by using systematic search algorithm implemented into BuildQSAR software within each descriptors subset firstly. Systematic search is a brute force method. In order to find the best three variable model that can be generated from the data set, for example, it is necessary to build and compare all possible three variable models. BuildQSAR can perform systematic search for the best model with one to five variables [21].

The most significant descriptors from each set were then included into single descriptors set followed by the systematic search procedure in order to confirm that the selected descriptors were the most optimal for describing the biological properties.

The statistical significance of the models generated was determined by examining the correlation coefficients *R* between the predicted and observed activities, the standard deviations *s*, the number of variables *n*, F-test ratio and the residuals analysis. The significant models selected were further undergone validation study by internal leave-one-out (LOO) cross-validation method. The predicted residual sums of squares standard deviation ($S_{PRESS}$), standard deviation error in prediction ($S_{DEP}$) and cross-validation coefficient $Q^2$ were used for the predictive ability validation of the QSAR-models. We

considered a QSAR model predictive, if the following conditions are satisfied [22]: $Q^2$>0.5; $R$>0.6. All of the above criteria are necessary to adequately assess the predictive ability of a QSAR model.

**Results and Discussion**

In our previous papers we reported synthesis of novel twenty nine $N^3$ substituted 5,7-dimethyl-3*H*-thiazolo[4,5-*b*]pyridine-2-one derivatives [3, 6]. These compounds have been evaluated for their free radical scavenging activity in terms of free-radical-scavenging activity percentage inhibition (% inhibition).

*Free radical scavenging activity evaluation*

The antioxidant activity of novel compounds was determined on basis of free radical scavenging activity of 2,2-diphenyl-1-picrylhydrazyl (DPPH) free radical. DPPH radical has found many applications due to its high stability in a methanolic solution and intense purple color. In its oxidized form, the DPPH radical has an absorbance maximum centered at a wavelength about 520 nm. The absorbance decreases when the radical is reduced by antioxidants. Its reduction affords 2,2-diphenyl-1-picrylhydrazine (DPPH-H), or the corresponding anion($DPPH^-$) in basic medium. The DPPH radical acts as a scavenger for other odd-electron species which afford *para*-substitution products at phenyl rings.

The DPPH method is described as a simple, rapid and convenient method for screening of many samples for radical scavenging activity. These advantages make the DPPH method interesting for testing newly synthesized compounds to scavenge radicals and to find out promising antioxidant drug candidates.

In the present paper we demonstrate modified spectrophotometric method makes use of the DPPH radical and its specific absorbance properties. The free-radical-scavenging activities of each compound were assayed using a stable DPPH and were quantified by decolorization the solution being mixed with DPPH at a wavelength of 517 nm. The absorbance of DPPH solution in ethanol (150 μmoles/L) was measured as 0.770.

The structures of novel $N^3$ substituted 5,7-dimethyl-3*H*-thiazolo[4,5-*b*]pyridine-2-one derivatives are depicted in Figure 1, while the substituent *R* structures and percentage of free-radical-scavenging activity expressed *via* percent inhibition are listed in Table 1.

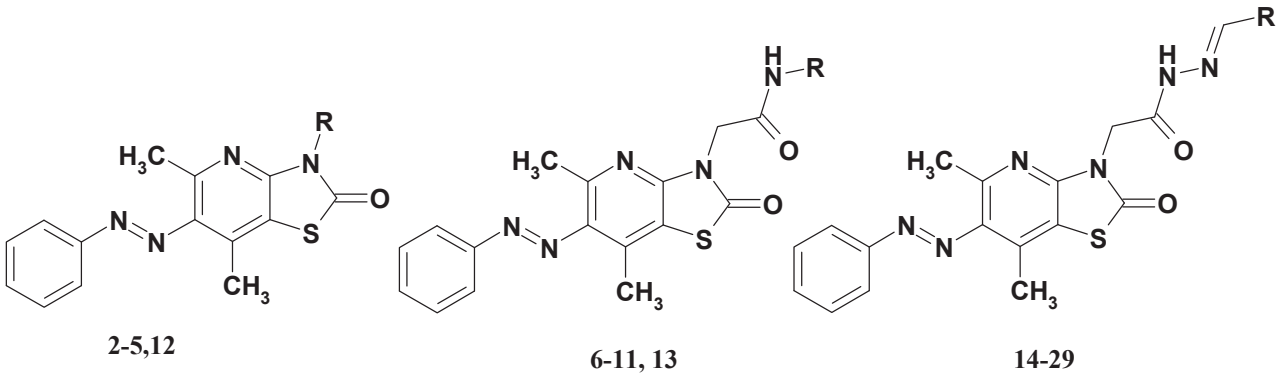


**Figure 1.** $N^3$ substituted 5,7-dimethyl-3*H*-thiazolo[4,5-*b*]pyridine-2-one scaffolds structure.

**Table 1.** $N^3$ substituents structures and free radical scavenging activity evaluation for 5,7-dimethyl-3*H*-thiazolo[4,5-*b*]pyridine derivatives.

| Compound ID | R | % Inhibition | Compound ID | R | % Inhibition |
|---|---|---|---|---|---|
| **1** | 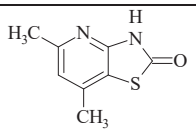 | 5.06 | **16** | 4-F-$C_6H_4$ | 22.43 |
| **2** | H | 8.05 | **17** | 4-Br-$C_6H_4$ | 8.18 |
| **3** | K | 7.14 | **18** | 4-Cl-$C_6H_4$ | 5.20 |
| **4** | $C_3H_7$ | 7.14 | **19** | 2-Cl-$C_6H_4$ | 7.00 |
| **5** | i-$C_3H_7$ | 5.22 | **20** | 4-$NO_2$-$C_6H_4$ | 7.14 |
| **6** | $C_6H_5$ | 7.00 | **21** | 3-$NO_2$-$C_6H_4$ | 8.31 |
| **7** | 4-$NO_2$-$C_6H_4$ | 5.04 | **22** | 3,4-$(CH_3O)_2$-$C_6H_3$ | 25.90 |
| **8** | 3-OH-$C_6H_4$ | 10.00 | **23** | 3-$CH_3O$-4-OH-$C_6H_3$ | 17.01 |
| **9** | 2-$NH_2$-$C_6H_4$ | 6.00 | **24** | 2-OH-5-Cl-C6H3 | 21.83 |
| **10** | 3-$CH_3$-C6H4 | 6.00 | **25** | 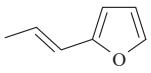 | 7.92 |
| **11** | 4-$C_2H_5$-$C_6H_4$ | 3.93 | **26** | 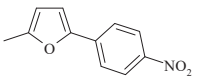 | 7.92 |
| **12** | $CH_2$-CO-O-$C_2H_5$ | 8.05 | **27** | 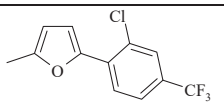 | 9.87 |
| **13** | $NH_2$ | 10.00 | **28** | 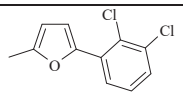 | 7.92 |
| **14** | 2-COOH-$C_6H_4$ | 11.02 | **29** | 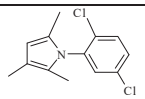 | 7.92 |
| **15** | 4-N-$(CH_3)_2$-$C_6H_4$ | 10.60 | | | |

The pharmacology screening allowed identifying three lead compounds whose free radical scavenging activities exceed that one for ascorbic acid their structures being depicted in Figure 2.

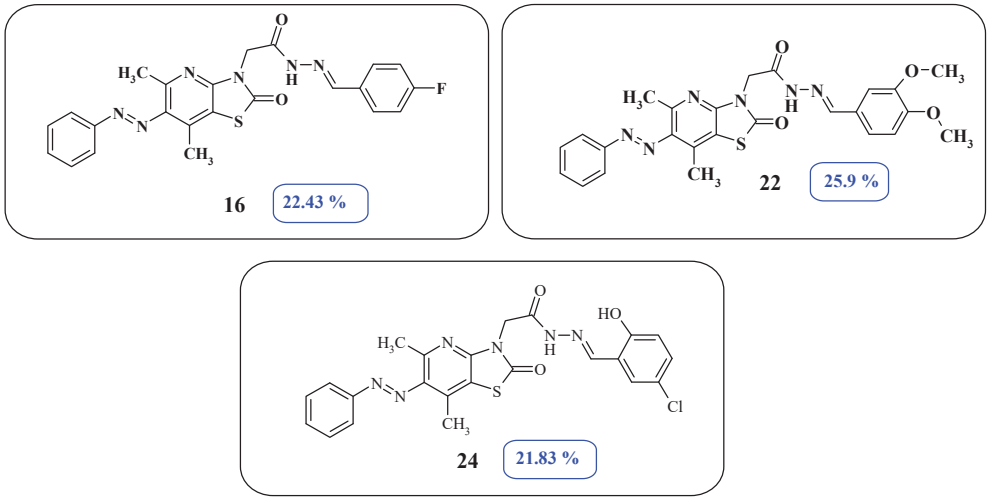


**Figure 2.** Structures of lead novel N³ substituted 5,7-dimethyl-3*H*-thiazolo[4,5-*b*]pyridine-2-one derivatives as free radical scavengers

In continuation with our work, and to develop a molecular pattern based on 3*H*-thiazolo[4,5-*b*]pyridine scaffold for the search and prediction on new compounds with antioxidant activity we thought it is essential to carry out a QSAR study for N³ substituted 5,7-dimethyl-3*H*-thiazolo[4,5-*b*]pyridine-2-one derivatives to perceive the importance of the molecular properties, which are critical in accentuating the biological activity. So 28 compounds (with 5,7-dimethyl-3*H*-thiazolo[4,5-*b*]pyridine-2-one potassium salt exception) were considered as experimental data set for the present study.

*Data sets preparation*

The 2*D* structures of the compounds under study have been drawn in ACD/ChemSketch. The drawn structures of 28 compounds (with the exception of 5,7-dimethyl-3*H*-thiazolo[4,5-*b*]pyridine-2-one potassium salt) were then converted into 3*D* modules using HyperChem 7.5 software. The energy of these 3*D* structures was minimized in HyperChem 7.5 using the Hamiltonian Austin Model 1 (AM1) procedure for closed shell systems. This ensured a well defined conformer relationship among the compounds of the study. All these energy minimized structures of compounds have been ported to DRAGON software for the computation of descriptors. This software offers more than 1600 descriptors from different perspectives corresponding to 0*D*-,1*D*-, 2*D*, 3*D* descriptor modules and module "Other". The outlined modules are comprised in their turn of different classes, namely, 0*D*: Constitutional descriptors, 1*D*: Functional group counts, Atom-centred fragments, 2*D*: Topological descriptors, Walk and path counts, Connectivity indices, Information indices, 2*D* autocorrelations, Edge adjacency indices, Burden eigenvalues, Topological charge indices, Eigenvalue-based indices, 3*D*: Randic molecular profiles, Geometrical descriptors, RDF descriptors, 3D-MoRSE descriptors, WHIM descriptors, GETAWAY descriptors, Others: charge descriptors, molecular properties. Some quantum chemical descriptors generated with HyperChem 7.5 software like the energies of the highest occupied molecular orbital ($E_{HOMO}$) and the lowest unoccupied molecular orbital ($E_{LUMO}$) together with octanol-water partition coefficient logP values for the compounds under study were incorporated into the data set.

*QSAR models development*

The combinatorial protocol in multiple linear regression (MLR) and partial least squares (PLS) procedures implemented into BuildQSAR software application have been used in the

present work for developing QSAR models. Multivariate regressions derived in this way relating the dependent variable as free radical scavenging inhibition percent to a number of independent variables (molecular descriptor) by using linear equations. This regression approach estimated the values of the regression coefficients by applying least square curve fitting-method.

The rule of thumb was applied to select number of descriptors in the models: the number of compounds used for the model generation ($n$) and the number of parameters under consideration ($M$) should undergo the ratio $n/M \geq 5$.

The statistical processing of variables selection for QSAR models obtaining was carried out by using systematic search algorithm within each descriptors class firstly as we reported earlier [23]. The most significant descriptors from each module class were then included into single descriptors set followed by the systematic search procedure in order to confirm that the selected descriptors were the most optimal for describing the biological properties. Pearson's correlation matrix was used to select the suitable descriptors for MLR analysis. Pearson's correlation matrix was performed on all descriptors by using "Correlation matrix" module available in BuildQSAR software.Cross-validation is a practical and reliable method for testing the significance of the variables over-fitting in order to avoid it.

The statistical significance of the models was determined by examining the correlation coefficients, the standard deviations, the number of variables, F-test ratio and the residuals analysis.

The significant models selected were further undergone validation study by internal leave-one-out (LOO) cross-validation method [24, 25]. In the LOO approach, each predicted compound is deleted from the $n$ compounds and its activity is computed. The square of LOO cross-validation coefficient $Q^2$ can be considered as a criterion of both predictive ability and robustness of the model as well as its stability. For a reliable model, the square of cross-validation coefficient $Q^2$ should be $\geq 0.5$ [26].

*Outcome of the QSAR studies*

QSAR modelling for antioxidant activity of novel $N^3$ substituted 5,7-dimethyl-3*H*-thiazolo[4,5-*b*]pyridine-2-ones resulted in predictive QSAR models development displaying the significant influence of atom-centred fragments and functional groups counts, topological and three-dimensional structure parameters, physicochemical properties, and quantum-chemical structure parameters on the free radical scavenging effect of the compounds.

Constitutional descriptors which are 0*D* subset ones are independent from molecular connectivity and conformations and refer to atom and bond type counts while we failed to develop any statistically significant QSAR model with this module descriptors at a required level of accuracy and predictivity.

The best bivariate QSAR models obtained with 1*D* descriptors for antioxidant activity of the compounds under study are given below with the statistical parameters of the regressions:

**% Inhibition = + 3.4984 C-037 + 7.5364 nArOR + 6.8777** **(1)**

($n$ = 28 ;$R$ = 0.719 ; $s$ = 3.986 ; $F$ = 13.358 ; $p$ = 0.0001 ; $Q^2$ = 0.427 ; $S_{Press}$ = 4.338 ; $S_{DEP}$ = 4.174);

**% Inhibition = + 3.4123 H-049 + 7.6401 nArOR + 6.7908** **(2)**

(n = 28 ;$R$ = 0.715 ; $s$ = 4.008 ; $F$ = 13.072 ; $p$ = 0.0001 ; $Q^2$ = 0.427 ; $S_{Press}$ = 4.339 ; $S_{DEP}$ = 4.175);

**% Inhibition = + 3.4123 N-074 + 7.6401 nArOR + 6.7908** **(3)**

(n = 28 ;$R$ = 0.715 ; $s$ = 4.008 ; $F$ = 13.072 ; $p$ = 0.0001 ; $Q^2$ = 0.427 ; $S_{Press}$ = 4.339 ; $S_{DEP}$ = 4.175).

The participated descriptors **C-037, H-049, N-074** and **nArOR** in models **1-3** are from Atom-centered fragments and Functional group counts classes of Dragon 1*D* module descriptors, respectively (Table 2).

**Table 2.** 1*D* module Dragon descriptors identification used in models **1-3**.

| Descriptors' symbol | Class | Definition and scope |
|---|---|---|
| **C-037** | Atom-centred fragments | Ar-CH=X |
| **H-049** | Atom-centred fragments | H attached to C3($sp^3$) / C2($sp^2$) / C3($sp^2$) / C3(sp) |
| **N-074** | Atom-centred fragments | R≡N / R=N- |
| **nArOR** | Functional group counts | Number of ethers (aromatic) |

The values of selected Dragon 1*D* module descriptors used for the models **1-3** obtaining are given in Table 3.

**Table 3.** Values of selected Dragon 1*D* module descriptors calculated for 5,7-dimethyl-3*H*-thiazolo[4,5-*b*]pyridine-2-one derivatives.

| Compound ID | C-037 | H-049 | N-074 | nArOR |
|---|---|---|---|---|
| **1** | 0 | 0 | 0 | 0 |
| **2** | 0 | 0 | 0 | 0 |
| **4** | 0 | 0 | 0 | 0 |
| **5** | 0 | 0 | 0 | 0 |
| **6** | 0 | 0 | 0 | 0 |
| **7** | 0 | 0 | 0 | 0 |
| **8** | 0 | 0 | 0 | 0 |
| **9** | 0 | 0 | 0 | 0 |
| **10** | 0 | 0 | 0 | 0 |
| **11** | 0 | 0 | 0 | 0 |
| **12** | 0 | 0 | 0 | 0 |
| **13** | 0 | 0 | 0 | 0 |
| **14** | 1 | 1 | 1 | 0 |
| **15** | 1 | 1 | 1 | 0 |
| **16** | 1 | 1 | 1 | 0 |

| | | | | |
|---|---|---|---|---|
| **17** | 1 | 1 | 1 | 0 |
| **18** | 1 | 1 | 1 | 0 |
| **19** | 1 | 1 | 1 | 0 |
| **20** | 1 | 1 | 1 | 0 |
| **21** | 1 | 1 | 1 | 0 |
| **22** | 1 | 1 | 1 | 2 |
| **23** | 1 | 1 | 1 | 1 |
| **24** | 1 | 1 | 1 | 0 |
| **25** | 0 | 1 | 1 | 0 |
| **26** | 1 | 1 | 1 | 0 |
| **27** | 1 | 1 | 1 | 0 |
| **28** | 1 | 1 | 1 | 0 |
| **29** | 1 | 1 | 1 | 0 |

Table 4 shows correlation matrix for the 1*D* module descriptors used in the resulting models **1-3**.

**Table 4.** Correlation matrix indicating inter-correlation between descriptors used in models **1-3.**

| | **C-037** | **H-049** | **N-074** | **nArOR** |
|---|---|---|---|---|
| **C-037** | 1.000 | | | |
| **H-049** | 0.930 | 1.000 | | |
| **N-074** | 0.930 | 1.000 | 1.000 | |
| **nArOR** | 0.244 | 0.227 | 0.227 | 1.000 |

C-037 descriptor was found to be correlated to H-049 and N-074 descriptors by 0.93. To overcome this limitation these three descriptors cann't be implemented into the same model.

Functional group counts molecular descriptors are based on the counting of chemical functional groups. The principal utility of molecular descriptors based on fragments is to obtain information about which fragments have positive (favorable) and which have undesirable influence on activity. This permits to reorient design of bioactive compounds in order to minimize the number of fragments with negative contribution and maximize the number of fragments with positive contribution.

Atom-centred fragments descriptors are simple molecular descriptors defined as the number of specific atom types in a molecule. They are calculated from the molecular composition and atom connectivities. Each atom type is an atom in the molecule described by its neighbouring atoms. Hydrogen and halogen atoms are classified by the hybridisation and oxidation

state of the carbon atom to which they are bonded; for hydrogens, heteroatoms attached to a carbon atom in some position are further considered. Carbon atoms are classified by their hybridisation state and depending on whether their neighbours are carbon or heteroatoms.

All 1*D* descriptors had shown positive influence on the activity. Thus we can suggest that the number of aromatic ether groups increasing in the molecules of substances under study, the presence of carbon-centered and nitrogen-centered fragments of Ar-CH=X and R≡ N/R=N- composition, and hydrogens number increasing, attached to carbon atoms in various hybridisation states would be favorable to the activity enhancing.

The next stage of QSAR studies workflow included the regressions development with 2*D* module descriptors. 2*D* descriptors, called graph invariants or topologic descriptors, are derived from molecular graph, and are conformationally independent. A QSAR study involving 2*D* descriptorsis quite simple for biological data interpretation in terms of different descriptors obtained from the two-dimensional structures of the compounds. In a congeneric series, where a relative study is being carried out, the 2*D* descriptors may play important role in deriving the significant correlations with biological activities of the compounds. Thus the novelty and importance of 2*D*-QSAR study is mainly due to its simplicity for the calculations of different descriptors and their interpretation (in physical sense) to explain the biological actions of compounds in a congeneric series.

The bivariate QSAR models **4-7** of the best statistics fitting while with the moderate predictive ability for antioxidant activity were obtained using 2*D* Autocorrelations and Connectivity indices classes' descriptors (Table 5):

**% Inhibition = + 79.4869 MATS6m - 47.0965 MATS1p + 13.8480** (**4**)
($n$ = 28; $R$ = 0.608 ;$s$ = 4.550 ; $F$ = 7.340 ; $p$ = 0.0031 ; $Q^2$ = 0.222 ; $S_{Press}$ = 5.057 ; $S_{DEP}$ = 4.866);

**% Inhibition = + 80.7866 MATS6m - 34.2618 MATS1v + 11.5837** (**5**)
($n$ = 28; $R$ = 0.606 ; $s$ = 4.560 ; $F$ = 7.256 ; $p$ = 0.0033 ; $Q^2$ = 0.216 ; $S_{Press}$ = 5.075 ; $S_{DEP}$ = 4.884);

**% Inhibition = - 75.0035 MATS4m - 37.2684 MATS2e + 7.5985** (**6**)
($n$ = 28; $R$ = 0.605 ;$s$ = 4.563 ; $F$ = 7.226 ; $p$ = 0.0033 ; $Q^2$ = 0.179 ; $S_{Press}$ = 5.196 ; $S_{DEP}$ = 5.000);

**% Inhibition = - 49.3437 MATS2e + 335.5611 X0A - 224.6141** (**7**)
($n$ = 28; $R$ = 0.598 ;$s$ = 4.595 ; $F$ = 6.952 ; $p$ = 0.0040 ; $Q^2$ = 0.146 ; $S_{Press}$ = 5.297 ; $S_{DEP}$ = 5.097).

**Table 5.** 2*D* module Dragon descriptors identification used in models **4-7**.

| Descriptors' symbol | Class | Definition and scope |
|---|---|---|
| **MATS4m** | 2*D* autocorrelations | Moran autocorrelation of lag 4 weighted by mass |
| **MATS6m** | 2*D* autocorrelations | Moran autocorrelation of lag 6 weighted by mass |

| | | |
|---|---|---|
| **MATS1p** | 2*D* autocorrelations | Moran autocorrelation of lag 1 weighted by atomic polarizabilities |
| **MATS1v** | 2*D* autocorrelations | Moran autocorrelation of lag 1 weighted by atomic van der Waals volumes |
| **MATS2e** | 2*D* autocorrelations | Moran autocorrelation of lag 2 weighted by Sanderson electronegativity |
| **X0A** | Connectivity indices | Average connectivity index of order 0 |

The values of selected Dragon 2*D* module descriptors used for the models **4-7** obtaining are given in Table 6.

**Table 6.** Values of selected Dragon 2*D* module descriptors calculated for 5,7-dimethyl-3*H*-thiazolo[4,5-*b*]pyridine-2-one derivatives.

| Compound ID | MATS4m | MATS6m | MATS1p | MATS1v | MATS2e | X0A |
|---|---|---|---|---|---|---|
| **1** | -0.043 | -0.128 | -0.002 | -0.098 | 0.258 | 0.726 |
| **2** | -0.019 | -0.009 | 0.07 | 0.027 | 0.131 | 0.706 |
| **4** | -0.052 | 0.005 | 0.057 | 0.003 | 0.136 | 0.713 |
| **5** | -0.043 | 0.009 | 0.058 | 0.009 | 0.149 | 0.719 |
| **6** | -0.071 | -0.070 | 0.021 | -0.033 | 0.120 | 0.703 |
| **7** | -0.096 | -0.059 | 0.145 | 0.137 | 0.132 | 0.713 |
| **8** | -0.074 | -0.059 | 0.009 | -0.044 | 0.041 | 0.708 |
| **9** | -0.074 | -0.069 | 0.014 | -0.042 | 0.090 | 0.708 |
| **10** | -0.067 | -0.073 | 0.022 | -0.029 | 0.130 | 0.708 |
| **11** | -0.060 | -0.071 | 0.024 | -0.025 | 0.136 | 0.708 |
| **12** | -0.088 | -0.076 | -0.006 | -0.088 | 0.130 | 0.719 |
| **13** | -0.077 | 0.005 | 0.078 | 0.025 | 0.095 | 0.719 |
| **14** | -0.100 | 0.017 | 0.046 | 0.003 | 0.157 | 0.713 |
| **15** | -0.060 | 0.013 | 0.035 | -0.022 | 0.097 | 0.713 |
| **16** | -0.085 | 0.014 | 0.051 | 0.010 | 0.010 | 0.708 |
| **17** | -0.018 | 0.016 | 0.070 | 0.050 | 0.079 | 0.708 |
| **18** | -0.063 | 0.022 | 0.080 | 0.042 | 0.053 | 0.708 |
| **19** | -0.061 | -0.016 | 0.080 | 0.042 | 0.053 | 0.708 |
| **20** | -0.099 | -0.004 | 0.179 | 0.175 | 0.129 | 0.713 |

| | | | | | | |
|---|---|---|---|---|---|---|
| **21** | -0.098 | 0.015 | 0.179 | 0.175 | 0.129 | 0.713 |
| **22** | -0.084 | 0.015 | -0.004 | -0.075 | -0.003 | 0.713 |
| **23** | -0.079 | 0.018 | 0.022 | -0.034 | -0.036 | 0.713 |
| **24** | -0.097 | 0.021 | 0.061 | 0.019 | -0.001 | 0.713 |
| **25** | -0.071 | 0.007 | 0.031 | -0.030 | -0.007 | 0.703 |
| **26** | -0.077 | 0.015 | 0.140 | 0.122 | 0.045 | 0.706 |
| **27** | -0.104 | -0.018 | 0.011 | -0.031 | 0.264 | 0.715 |
| **28** | -0.079 | -0.028 | 0.052 | 0.001 | 0.063 | 0.706 |
| **29** | -0.067 | -0.086 | 0.058 | 0.012 | -0.016 | 0.714 |

Table 7 shows correlation matrix for the 2*D* module Dragon descriptors used in QSAR models **4-7**.

**Table 7.** Correlation matrix indicating inter-correlation between descriptors used in models **4-7**.

| | **MATS4m** | **MATS6m** | **MATS1v** | **MATS2e** | **MATS1p** | **X0A** |
|---|---|---|---|---|---|---|
| **MATS4m** | 1.000 | | | | | |
| **MATS6m** | 0.097 | 1.000 | | | | |
| **MATS1v** | 0.205 | 0.392 | 1.000 | | | |
| **MATS2e** | 0.071 | 0.363 | 0.032 | 1.000 | | |
| **MATS1p** | 0.191 | 0.369 | 0.290 | 0.018 | 1.000 | |
| **X0A** | 0.093 | 0.190 | 0.159 | 0.440 | 0.085 | 1.000 |

QSAR models **4-7** were derived with Moran autocorrelation descriptors MATS4m, MATS6m, MATS1p, MATS1v and MATS2e. These descriptors are calculated from the molecular graph by summing the products of atoms weight of terminal atoms of all the paths of the considered path length (the lag).

The Moran autocorrelation descriptors ($MATS_{dw}$) are given by:

$$I(d) = \frac{\frac{1}{\Delta} \cdot \sum_{i=1}^{A} \sum_{j=1}^{A} \delta_{ij} \cdot (\omega_i - \overline{\omega}) \cdot (\omega_j - \overline{\omega})}{\frac{1}{A} \cdot \sum_{i=1}^{A} (\omega_i - \overline{\omega})^2}$$

where $\overline{\omega}$ is the average value of the property for the molecule, and $\Delta = \sum \delta_{ij}$ is the number of vertex pairs at distance equal to *d*. The computation of these descriptors involved summing different autocorrelation functions corresponding to different fragment lengths, thereby leading to different autocorrelation vectors according to the lengths of the structural fragments. Also a weighting component in terms of a physicochemical property has been considered, and therefore these descriptors address the topology of the structure or parts of its merged with a selected physicochemical property [27].

The presence of lags 1, 2, 4 and 6 2*D* Autocorrelations in QSAR regressions **4-7** may be reviewed as the association of activity in

formation content with structural fragments of such size. It should be noted that mass weighted Moran auto-correlation coefficient MATS6m made a positive contribution to the free radical scavenging activity while the mass weighted Moran auto-correlation coefficient MATS4m made a negative contribution. Additionally polarizability and van der Waals volumes weighted Moran auto-correlation coefficients with lag 1 (MATS1p and MATS1v) as well as electronegativity weighted MATS2e made negative contributions. In another words, the presence of structural fragments of lag 6, in which the terminal atoms have high atomic weight would be preferable for the antioxidant activity enhancing while the presence of structural fragments of lag 4 with the heavy terminal atoms would have undesirable influence on activity. The presence of structural fragments of lags 1 and 2, in which the terminal atoms have high polarizability, van der Waals volume and electronegativity, respectively, would be also undesirable.

The positive contributions to the antioxidant activity were made with Average connectivity index of order 0 descriptor X0A (model **7**). Randic connectivity indices descriptors may be interpreted as a contribution of one molecule into the bimolecular interaction which may occur as a result of two identical molecules intersection. Thus, the interpretation of these models may propose the increase in antioxidant activity of the compounds in case of the minimal vertices degrees for each two adjacent vertices of the molecular graph that is when all bonds can participate in the intersection within the intermolecular interactions. This interpretation excludes the presence of branched substituents in the molecules of antioxidant potential.

On the next stage of the QSAR modeling workflow three-variables regressions **8-10** were developed with the incorporation of 3*D* module descriptors including 3*D*-MoRSE and WHIM classes ones (Table 8). The best QSAR models obtained with 3*D* descriptors for antioxidant activity are given below with the statistical parameters of the regressions:

**% Inhibition = + 7.9626 Mor15e + 26.0062 Mor26e + 339.3781 G1p - 67.6403(8)**
($n$ = 28 ;$R$ = 0.817 ; $s$ = 3.376 ; $F$ = 16.021 ; $p$< 0.0001 ; $Q^2$ = 0.555 ; $S_{Press}$ = 3.901 ; $S_{DEP}$ = 3.678);

**% Inhibition = + 7.9528 Mor15e + 10.7712 Mor23e + 18.8572 Mor26e - 0.9431(9)**
($n$ = 28 ;$R$ = 0.799 ; $s$ = 3.520 ; $F$ = 14.099 ; $p$ < 0.0001 ; $Q^2$ = 0.508 ; $S_{Press}$ = 4.103 ; $S_{DEP}$ = 3.868);

**% Inhibition = + 8.4116 Mor15u + 26.3608 Mor26e + 338.4023 G1p - 67.4650(10)**
($n$ = 28 ;$R$ = 0.792 ; $s$ = 3.569 ; $F$ = 13.495 ; $p$< 0.0001 ; $Q^2$ = 0.505 ; $S_{Press}$ = 4.115 ; $S_{DEP}$ = 3.880).

**Table 8.** 3*D* module Dragon descriptors identification used in models **8-10**.

| Descriptors' symbol | Class | Definition and scope |
|---|---|---|
| **Mor15u** | 3D-MoRSE | 3D-MoRSE – signal 15 / unweighted |
| **Mor15e** | 3D-MoRSE | 3D-MoRSE – signal 15 / weighted by atomic Sanderson electronegativity |

| | | |
|---|---|---|
| **Mor23e** | 3D-MoRSE | 3D-MoRSE – signal 23 / weighted by atomic Sanderson electronegativity |
| **Mor26e** | 3D-MoRSE | 3D-MoRSE – signal 26 / weighted by atomic Sanderson electronegativity |
| **G1p** | WHIM | 1st component directional WHIM index / weighted by atomic polarizabilities |

The values of selected Dragon 3*D* module descriptors used for the models **8-10** obtaining are given in Table 9.

**Table 9.** Values of selected Dragon 3*D* module descriptors calculated for 5,7-dimethyl-3*H*-thiazolo[4,5-*b*]pyridine-2-one derivatives.

| Compound ID | Mor15u | Mor15e | Mor23e | Mor26e | G1p |
|---|---|---|---|---|---|
| **1** | 0.170 | 0.169 | -0.072 | 0.247 | 0.188 |
| **2** | 0.547 | 0.611 | -0.519 | 0.467 | 0.167 |
| **4** | 0.430 | 0.502 | -0.921 | 0.768 | 0.157 |
| **5** | 0.380 | 0.434 | -0.976 | 0.512 | 0.166 |
| **6** | 0.683 | 0.741 | -0.946 | 0.695 | 0.161 |
| **7** | 0.802 | 0.827 | -0.826 | 0.504 | 0.160 |
| **8** | 0.786 | 0.859 | -0.855 | 0.632 | 0.151 |
| **9** | 1.273 | 1.382 | -0.934 | 0.445 | 0.160 |
| **10** | 0.647 | 0.682 | -0.934 | 0.753 | 0.149 |
| **11** | 0.632 | 0.682 | -1.087 | 0.608 | 0.147 |
| **12** | 0.495 | 0.545 | -0.488 | 0.627 | 0.155 |
| **13** | 0.756 | 0.812 | -0.565 | 0.531 | 0.157 |
| **14** | 1.018 | 1.116 | -0.952 | 0.669 | 0.147 |
| **15** | 1.613 | 1.707 | -0.961 | 0.795 | 0.145 |
| **16** | 1.008 | 1.128 | -0.938 | 0.851 | 0.176 |
| **17** | 1.047 | 1.139 | -0.887 | 0.721 | 0.149 |
| **18** | 0.878 | 0.935 | -1.016 | 0.659 | 0.149 |
| **19** | 0.837 | 0.882 | -0.994 | 0.749 | 0.149 |
| **20** | 1.489 | 1.704 | -1.061 | 0.451 | 0.147 |

| | | | | | |
|---|---|---|---|---|---|
| **21** | 0.959 | 1.001 | -0.876 | 0.680 | 0.157 |
| **22** | 1.234 | 1.465 | -0.561 | 0.920 | 0.145 |
| **23** | 1.416 | 1.613 | -0.753 | 0.723 | 0.153 |
| **24** | 1.348 | 1.496 | -0.879 | 0.683 | 0.158 |
| **25** | 0.840 | 0.831 | -1.002 | 0.603 | 0.149 |
| **26** | 1.224 | 1.302 | -1.535 | 0.626 | 0.144 |
| **27** | 1.923 | 2.111 | -1.134 | 0.257 | 0.158 |
| **28** | 1.621 | 1.714 | -1.238 | 0.407 | 0.156 |
| **29** | 1.169 | 1.224 | -0.936 | 0.714 | 0.149 |

In Table 10 correlation matrix for the 3*D* module Dragon descriptors used in the QSAR models **4-7** is given.

**Table 10.** Correlation matrix indicating inter-correlation between descriptors used in models **8-10**.

| | **Mor15u** | **Mor15e** | **Mor23e** | **Mor26e** | **G1p** |
|---|---|---|---|---|---|
| **Mor15u** | 1.000 | | | | |
| **Mor15e** | 0.296 | 1.000 | | | |
| **Mor23e** | 0.299 | 0.368 | 1.000 | | |
| **Mor26e** | 0.013 | 0.004 | 0.115 | 1.000 | |
| **G1p** | 0.414 | 0.404 | 0.242 | 0.243 | 1.000 |

3*D* molecular descriptors had been shown to be very useful in QSAR problems in order to perform a rational analysis of different pharmacological activities [27].

3D-MoRSE (3*D*-Molecule Representation of Structures based on Electron diffraction) descriptors are based on the idea of obtaining information from the 3*D* atomic coordinates by the transforming used in electronic diffraction studies for preparing theoretical scattering curves [27]. A generalized scattering function, called the molecular transform, can be used as the functional basis for deriving, from a known molecular structure, the specific analytical relationship of both X-ray and electron diffraction. The general molecular transform is:

$$G(s) = \sum_{i=1}^{A} f_i \cdot \exp(2\pi_i \cdot r_i \cdot s)$$

where $s$ represents the scattering in various directions by a collection of $A$ atoms located at points $r_i$; $f_i$ is a form factor taking into account the direction dependence of scattering from a spherical body of finite size. The scattering value, $s$, measures the scattering angle as: $s = 4\pi \cdot \sin(\theta/2)/\lambda$, where $\theta$ is the scattering angle and $\lambda$ is the wavelength of the electron beam.

The equation for $G(s)$ is usually used in the modified form. On substituting the form factor by the atomic property $w$, considering the

molecule to be rigid and setting the instrumental constant equal to unity, the following expression is obtained:

$$Mor(s,w) = I(s,w) = \sum_{i=2}^{n}\sum_{j=1}^{i-1} w_i w_j \sin(sr_{ij})\, /(sr_{ij}),$$

where $I$ ($s$,$w$) is the scattered electron intensity, $w$ is an atomic property, chosen as the atomic number, $r_{ij}$ are the interatomic distances between the $i^{th}$ and $j^{th}$ atoms, and $A$ is the number of atoms. For atomic weightings $w$, various physicochemical properties such as atomic mass, partial atomic charge, or atomic polarizability are considered.

To obtain uniform length descriptors, the intensity distribution $I(s)$ is made discrete, its value being calculated as a sequence of evenly distributed values, e.g. 32 or 64 values in the range of 1-31 $Å^{-1}$. Clearly, the more values are chosen, the finer becomes the resolution in the representation of the molecule.

The 3D-MoRSE descriptors have been shown to have good modeling power for different biological and physicochemical properties and can be used even for the simulation of infrared spectra.

3D-MoRSE descriptors 3D-MoRSE – signal 15/unweighted, 3D-MoRSE – signal 15/weighted by atomic Sanderson electronegativity, 3D-MoRSE – signal 23/weighted by atomic Sanderson electronegativity and 3D-MoRSE – signal 26/weighted by atomic Sanderson electronegativity were incorporated into all 3*D* model regressions for antioxidant activity of 5,7-dimethyl-3*H*-thiazolo[4,5-*b*]pyridine-2-ones making the positive contribution into the activity enhancing.Thus, the increase in activity occurred when the electron beam scattering with the group of atoms would be mainly on account of groups of atoms with high electronegativities situated at the Euclidean distance of 15, 23 or 26 Å between them, or a group of any atoms located at a distance of 15 Å.

WHIM descriptors (Weighted Holistic Invariant Molecular descriptors) are geometrical descriptors based on statistical indices calculated on the projections of the atoms along principal axes [27]. WHIM descriptors are built in such a way to capture relevant molecular 3*D* information regarding molecular size, shape, symmetry and atom distribution with respect to invariant reference frames. They are divided into two main classes: directional WHIM descriptors and global WHIM descriptors.

Within the WHIM approach, a molecule is seen as a configuration of points (the atoms) in the three-dimensional space defined by the Cartesian axes (x, y, z). To obtain a unique reference frame, principal axes of the molecule are calculated. Projections of the atoms along each of the principal axes are then performed and their dispersion and distribution around the geometric center are evaluated. Thus the WHIM approach can be viewed as a generalization of searching for the principal axes with respect to the defined atomic property (the weighting scheme).

The axial symmetry of the atoms in the molecule by the new internal coordinate axes (axes of the three major components) can be calculated by the equation:

$$\gamma_m = \left\{1 - \left[\frac{n_s}{A}\cdot\log_2\frac{n_s}{A} + n_a\cdot\left(\frac{1}{A}\cdot\log_2\frac{1}{A}\right)\right]\right\}^{-1},\ m = 1, 2, 3,$$

where $n_s$ is the number of symmetrical atoms along the principal components axis, $n_a$ is the number of unsymmetrical atoms, $A$ – the number of atoms in the molecule.

Then the index of overall symmetry of the molecule is calculated as follows:

$$G = (\gamma_1 \cdot \gamma_2 \cdot \gamma_3)^{1/3}$$

Overall symmetry index values are directing to 1 if the atoms in the molecule are symmetrically situated along each axis and 0 if the atoms have low symmetry with respect to at least one of the principle component axes.

Derived models **8** and **10** for antioxidant activity of the compounds under study comprised 1st component directional WHIM index weighted by atomic polarizabilities (G1p) which

made a positive contribution into the activity. This fact could be related to the importance in the strong symmetry keeping with the atoms possessing high polarizability, like Oxygen or Chlorine, along the 1st principle component axe.

The incorporation of the most significant and relevant descriptors from all modules and quantum chemical descriptors generated with HyperChem software into one data set (Table 11) allowed to carry out QSAR modeling for antioxidant activity of 5,7-dimethyl-3*H*-thiazolo[4,5-*b*]pyridine-2-one derivatives with the mixed regressions **11-15** obtaining:

**% Inhibition = + 4.6354 O-060 + 24.2326 Mor26e + 15.8546 Mor29e - 1.2400** (**11**)
($n$ = 28 ; $R$ = 0.782 ; $s$ = 3.644 ; $F$ = 12.618 ; $p$< 0.0001 ; $Q^2$ = 0.505 ; $S_{Press}$ = 4.116 ; $S_{DEP}$ = 3.880);

**% Inhibition = + 8.7796 nArOR + 0.0344 logP + 17.8271 MATS6m + 7.8340** (**12**)
($n$ = 26 ; $R$ = 0.925 ; $s$ = 1.772 ; $F$ = 43.705 ; $p$< 0.0001 ; $Q^2$ = 0.820 ; $S_{Press}$ = 1.983 ; $S_{DEP}$ = 1.861);

**% Inhibition = + 1.3704 C-037 + 8.8107 nArOR - 0.5446 $E_{LUMO}$ + 6.2879** (**13**)
($n$ = 26 ; $R$ = 0.923 ; $s$ = 1.798 ; $F$ = 42.264 ; $p$< 0.0001 ; $Q^2$ = 0.773 ; $S_{Press}$ = 2.226 ; $S_{DEP}$ = 2.088);

**% Inhibition = + 1.4325 H-049 + 8.8246 nArOR - 0.3882 $E_{LUMO}$ + 6.3732** (**14**)
($n$ = 26 ; $R$ = 0.924 ; $s$ = 1.786 ; $F$ = 42.943 ; $p$< 0.0001 ; $Q^2$ = 0.775 ; $S_{Press}$ = 2.220 ; $S_{DEP}$ = 2.082);

**% Inhibition = + 1.4325 N-074 + 8.8246 nArOR - 0.3882 $E_{LUMO}$ + 6.3732** (**15**)
($n$ = 26 ; $R$ = 0.924 ; $s$ = 1.786 ; $F$ = 42.943 ; $p$< 0.0001 ; $Q^2$ = 0.775 ; $S_{Press}$ = 2.220 ; $S_{DEP}$ = 2.082).

**Table 11.** All modules Dragon descriptors and quantum chemical descriptors identification used in models **11-15**.

| Descriptors' symbol | Module | Class | Definition and scope |
|---|---|---|---|
| **O-060** | 1*D* | Atom-centred fragments | Alk-O-Ar / Ar-O-Ar / R..O..R / R-O-C=X |
| **Mor29e** | 3*D* | 3D-MoRSE | 3D-MoRSE – signal 29 / weighted by atomic Sanderson electronegativity |
| $E_{LUMO}$ | HyperChem | Quantum chemical | Energy of lowest unoccupied molecular orbital, eV |
| **logP** | HyperChem | Molecular properties | Octanol-water partition coefficient (HyperChem) |

The values of selected all modules Dragon descriptors and quantum chemical descriptors used for the models **11-15** generation are given in Table 12.

**Table 12.** Values of selected all modules Dragon descriptors and quantum chemical descriptos calculated for 5,7-dimethyl-3*H*-thiazolo[4,5-*b*]pyridine-2-one derivatives.

| Compound ID | O-060 | Mor29e | $E_{LUMO}$ | logP |
|---|---|---|---|---|
| **1** | 0 | -0.142 | -0.43688 | 2.00 |
| **2** | 0 | -0.095 | -1.06975 | 4.30 |
| **4** | 0 | -0.542 | -1.01197 | 5.36 |
| **5** | 0 | -0.374 | -1.01033 | 5.76 |
| **6** | 0 | -0.313 | -1.14601 | 5.16 |
| **7** | 0 | -0.138 | -1.32792 | 1.25 |
| **8** | 0 | -0.210 | -1.18862 | 4.87 |
| **9** | 0 | -0.256 | -1.15078 | 4.37 |
| **10** | 0 | -0.593 | -1.15312 | 5.62 |
| **11** | 0 | -0.554 | -1.15183 | 6.02 |
| **12** | 1 | -0.478 | -1.10208 | 4.47 |
| **13** | 0 | -0.321 | -1.16033 | 3.22 |
| **14** | 0 | -0.266 | -1.06755 | 5.47 |
| **15** | 0 | -0.521 | -0.94406 | 6.04 |
| **16** | 0 | -0.220 | -1.21445 | 5.91 |
| **17** | 0 | -0.248 | -1.15841 | 6.57 |
| **18** | 0 | -0.328 | -1.21250 | 6.29 |
| **19** | 0 | -0.475 | -1.11631 | 6.29 |
| **20** | 0 | -0.169 | -1.31088 | 5.73 |
| **21** | 0 | -0.137 | -1.22548 | 1.86 |
| **22** | 2 | -0.274 | -1.04791 | 5.27 |
| **23** | 1 | -0.519 | -1.17514 | 5.58 |
| **24** | 0 | -0.273 | -1.21068 | 6.01 |
| **25** | 1 | -0.587 | -1.16902 | 3.30 |
| **26** | 1 | -0.623 | -1.16896 | 0.44 |
| **27** | 1 | -0.071 | -1.23621 | 5.75 |

| | | | | |
|---|---|---|---|---|
| **28** | 1 | -0.272 | -1.07463 | 6.10 |
| **29** | 0 | -0.705 | -0.95136 | 6.09 |

Table 13 shows correlation matrix for the all modules Dragon descriptors and quantum chemical descriptors used for QSAR models **11-15** construction.

**Table 13.** Correlation matrix indicating inter-correlation between descriptors used in models **11-15**.

| | **O-060** | $E_{LUMO}$ | **logP** | **Mor29e** |
|---|---|---|---|---|
| **O-060** | 1.000 | | | |
| $E_{LUMO}$ | 0.047 | 1.000 | | |
| **logP** | 0.101 | 0.087 | 1.000 | |
| **Mor29e** | 0.125 | 0.092 | 0.130 | 1.000 |

Analysis of the residuals and standard deviations of residuals for regressions **12** and **15** (Table 14) allowed identifying compounds **16** and **24** as the significant outliers and they were excluded from the data set.

**Table 14.** Observed and predicted antioxidant activities, residuals and standard deviations of residuals for the compounds according to the QSAR models **12** and **15**.

| **Compound ID** | **Observed activity, %** | **Model 12** | | | **Model 15** | | |
|---|---|---|---|---|---|---|---|
| | | **Predicted activity, %** | **Residual** | **St. dev. of resid.** | **Predicted activity, %** | **Residual** | **St. dev. of resid.** |
| **1** | 5.060 | 2.494 | 2.566 | 0.704 | 4.883 | 0.177 | 0.043 |
| **2** | 8.050 | 8.570 | -0.520 | -0.143 | 6.773 | 1.277 | 0.315 |
| **4** | 7.140 | 8.777 | -1.637 | -0.449 | 6.600 | 0.540 | 0.133 |
| **5** | 5.220 | 5.237 | -0.017 | -0.005 | 6.595 | -1.375 | -0.339 |
| **6** | 7.000 | 10.639 | -3.639 | -0.999 | 7.000 | 0.000 | 0.000 |
| **7** | 5.040 | 8.785 | -3.745 | -1.028 | 7.543 | -2.503 | -0.617 |
| **8** | 10.000 | 10.746 | -0.746 | -0.205 | 7.128 | 2.872 | 0.708 |
| **9** | 6.000 | 5.485 | 0.515 | 0.141 | 7.015 | -1.015 | -0.250 |

| | | | | | | | |
|---|---|---|---|---|---|---|---|
| **10** | 6.000 | 7.605 | -1.605 | -0.440 | 7.022 | -1.022 | -0.252 |
| **11** | 3.930 | 4.710 | -0.780 | -0.214 | 7.018 | -3.088 | -0.761 |
| **12** | 8.050 | 11.011 | -2.961 | -0.812 | 6.869 | 1.181 | 0.291 |
| **13** | 10.000 | 6.538 | 3.462 | 0.950 | 7.043 | 2.957 | 0.728 |
| **14** | 11.020 | 10.754 | 0.266 | 0.073 | 9.959 | 1.061 | 0.261 |
| **15** | 10.600 | 9.765 | 0.835 | 0.229 | 9.590 | 1.010 | 0.249 |
| **16** | 22.430 | 15.894 | 6.536 | 1.793 | 10.397 | 12.033 | 2.964 |
| **17** | 8.180 | 12.300 | -4.120 | -1.130 | 10.230 | -2.050 | -0.505 |
| **18** | 5.200 | 9.529 | -4.329 | -1.188 | 10.392 | -5.192 | -1.279 |
| **19** | 7.000 | 9.379 | -2.379 | -0.653 | 10.104 | -3.104 | -0.765 |
| **20** | 7.140 | 7.009 | 0.131 | 0.036 | 10.685 | -3.545 | -0.873 |
| **21** | 8.310 | 13.066 | -4.756 | -1.305 | 10.430 | -2.120 | -0.522 |
| **22** | 25.900 | 25.981 | -0.081 | -0.022 | 25.392 | 0.508 | 0.125 |
| **23** | 17.010 | 12.687 | 4.323 | 1.186 | 18.026 | -1.016 | -0.250 |
| **24** | 21.830 | 10.983 | 10.847 | 2.976 | 10.386 | 11.444 | 2.819 |
| **25** | 7.920 | 8.701 | -0.781 | -0.214 | 10.262 | -2.342 | -0.577 |
| **26** | 7.920 | 8.687 | -0.767 | -0.211 | 10.262 | -2.342 | -0.577 |
| **27** | 9.870 | 8.497 | 1.373 | 0.377 | 10.462 | -0.592 | -0.146 |
| **28** | 7.920 | 8.946 | -1.026 | -0.281 | 9.980 | -2.060 | -0.507 |
| **29** | 7.920 | 4.885 | 3.035 | 0.833 | 9.612 | -1.692 | -0.417 |

The positive contributions to the antioxidant activity were made with 1*D* module descriptor O-060 (model **11**), which belongs to the Atom-centred fragments class. Thus the presence of the oxygen-centered fragments with the composition of Alk-O-Ar / Ar-O-Ar / R..O..R / R-O-C=X in the molecules of the compounds under study would enhance the activity.

According to the free-radical-scavenging activity QSAR model **12** HyperChem generated octanol-water partition coefficient log*P* make positive contribution to potency of inhibition, so the decreasing of hydrophilicity enhanced the antioxidant activity of the compounds.

The negative sign of the regression coefficients for the lowest unoccupied molecular orbital energy $E_{LUMO}$ in models **13-15** suggested that the percent inhibition of radical reactive species with thiazolo[4,5-*b*]pyridines would become stronger with their electrons acceptor ability increasing.

## Conclusions

QSAR modeling for the series of novel N[3] substituted 5,7-dimethyl-3*H*-thiazolo[4,5-*b*]pyridine-2-one derivatives was carried out and the MLR regressions were developed involving integration of the structural fragments, quantum-chemical molecular parameters, physicochemical molecular information and atom and bond types counts making it possible to traverse backward from a large amount of structural features into a single number to structural interpretation. The analysis of the QSAR

models derived with multiply linear regression technique revealed the antioxidant activity enhancing with the hydrophilic properties decreasing and electrons acceptor ability increasing of the compounds. Moreover small aromatic molecules containing certain oxygen- and nitrogen-centered fragments and ethers aromatic groups without bulky and branched substituent or atoms with high electronegativity are supposed to possess stronger free radical scavenging activity.

It had been demonstrated statistically that achieved QSAR models could be used for virtual screening of novel 3*H*-thiazolo[4,5-*b*]pyridine-2-one derivatives in order to identify antioxidant agents based on the same congeneric series.

**References**

1. Sayed HH, Morsy EMH, Kotb ER. Facile novel synthesis and reactions of thiazolidin-4-one derivatives for antimicrobial agents. Synth. Commun 2010; 40(18): 2712-2722.

2. Lee YR, Dong JK, Inhee MJ, Yoo KH. Synthesis of thia(oxa)zolopyridines and their inhibitory activities for β-Amyloid Fibrillization. Bull. Korean Chem. Soc. 2008; 29(12): 2331-2336.

3. Chaban TI, Klenina OV, Zimenkovsky BS, Chaban IG,Ogurtsov VV, Shelepeten LS. Synthesis of novel thiazolo[4,5-*b*]pyridines as potential biologically active substances. Der Pharma Chemica 2016; 8(19):534-542.

4. Chaban T, Klenina O, Drapak I, Ogurtsov V, Chaban I, Novikov V. Synthesis of some novel thiazolo[4,5-*b*]pyridines and their tuberculostatic activity evaluation. Chem. & Chem. Techn. 2014; 89: 287-292.

5. Chaban TI, Panchuk RR, Klenina OV, Skorokhyd NR, Ogurtsov VV, Chaban IG. Synthesis and evaluation of antitumor activity of some thiazolo[4,5-*b*] pyridines. Biopolymers and Cell. 2012; 28: 389-396.

6. Chaban TI, Ogurtsov VV, Chaban IG, Klenina OV, Komarytsia JD. Synthesis and antioxidant activity evaluation of novel 5,7-dimethyl-3*H*-thiazolo[4,5-*b*]pyridines. Phosphorus, Sulfur Silicon Relat. Elem. 2013; 188: 1611-1620.

7. Klenina O, Drapak I, Chaban T, Ogurtsov V, Chaban I, Golos I. QSAR studies of some thiazolo[4,5-*b*]pyridines as novel antioxidant agents: enhancement of activity by some molecular structure parameters. Chem. & Chem. Techn. 2013; 7: 397-404.

8. Marzoog S, Al-Thebeiti. Synthesis of some new thiazolo[3,2-*a*]pyridines and related heterocyclic systems. Il Farmaco 2000; 55:109-118.

9. Walczyn´ski K, ZuiderveldOP, Timmerman H. Non-imidazole histamine H3 ligands. Part III. New 4-n-propylpiperazines as non-imidazole histamine H3-antagonists. European Journal of Medicinal Chemistry. 2005; 40: 15–23.

10. Rao AU, PalaniA, Chen X, Huang Y, Aslanian RG, West Jr RE, Williams SM, Wu RL, Hwa J, Sondey C, Lachowicz J. Bioorg. Med. Chem. Lett 2009 ; 19 (21): 6176-6180.

11. Kulkarni SS, Newman AH. Discovery of heterobicyclic templates for novel metabotropic glutamate receptor subtype 5 antagonists. Bioorg. Med. Chem. Lett. 2007;17: 2987-2992.

12. Lin R, Johnson SG, Connolly PJ, Wetter SK, Binnun E, Hughes TV, Murray WV, Pandey NB, Moreno-Mazza SJ, Adams M, Fuentes-Pesquera AR,Middleton SA. Synthesis and evaluation of 2,7-diamino-thiazolo[4,5-*d*]pyrimidine analogues as anti-tumor epidermal growth factor receptor (EGFR) tyrosine kinase inhibitors. Bioorg. Med. Chem. Lett. 2009; 19: 2333-2337.

13. Bebernitz GR, Beaulieu V, Dale BA, Deacon R, Duttaroy A, Gao J. Investigation of functionally liver selective glucokinase activators for the treatment of type 2 diabetes. J Med Chem. 2009;52:6142–6152.

14. Lozynska L, Tymoshuk O, Chaban T. Spectrophotometric studies of 4-[n'-(4-imino-2-oxo-thiazolidin-5-ylidene) - hydrazino]-benzenesulfonic acid as a reagent for the determination of Palladium. Acta Chim. Slov.2015; 62: 159-167.

15. Kubinui H. QSAR: Hansch analysis and related approaches. VCH: New York: 1993.

16. Chaban TI; Zimenkovskii BS, Komaritsa JD, ChabanIG. Reaction of 4-iminothiazolidin-2-one with acetylacetone. Rus. J. Org.Chem. 2012; 48 (2): 268−272.

17. Blois MS. Antioxidant determinations by the use of a stable free radical. Nature 1958; 181: 1199-1200.

18. Molyneux PJ.The use of stable free radical diphenylpicrylhydrazyl (DPPH) for estimating antioxidant activity. Sci. Technol. 2004; 26: 211-219.

19. Huper Cube, Inc.: http://www.hyper-.com HyperChem software. HuperCube, Inc. 1115 NW 4th Street, Gainesville, Fl 32601 USA http://www.hyper.com.

20. VCCLAB, Virtual Computational Chemistry Laboratory, http://www.vcclab.org: 2005.

21. De Oliviera DB, Gaudio C. Build-QSAR. Quantitative Structure – Activity Relationships, 2000; 19 (6): 599-601.

22. Golbraikh A, Tropsha A. Beware of $q^2$. J. Mol. Graphics Model.2002; 20: 269–276.

23. Suleiman MM, Isaev SG, Klenina OV, Ogurtsov VV. Synthesis, biological activity evaluation and QSAR studies of novel 3-(amino-oxalyl-amino)- and 3-(carbamoyl-propionylamino)-2-phenylamino-benzoic acid derivatives. J.Chem.Pharm.Res. 2014; 6(5):1219-1235.

24. Schaper KJ. Free-wilson-type analysis of non-additive substituent effects on THPB dopamine receptor affinity using artificial neural networks. Quant. Struct. Act. Relat. 1999; 18: 354-360.

25. Tetko IV, Tanchuk VY, Villa AE. Prediction of n-octanol/water partition coefficients from PHYSPROP database using artificial neural networks and E-state indices. J Chem Inf Comput Sci 2001; 41:1407–1421.

26. Clark M.; CramerRD. III The probability of chance correlation using partial least squares (PLS).Quant. Struct.-Act. Relat. 1993;12(2): 137-145.

27. Todeschini R, Consonni V. Molecular descriptors for chemoinformatics. Weinheim (Germany), WILEY-VCH: 2009.

**Corresponding author:**
Department of General, Bioinorganic, Physical and Colloidal Chemistry
Danylo Halytsky Lviv National Medical University, Ukraine
Pekarska 69, Lviv, 79010, Ukraine
*olena_klenina@yahoo.com* (O. Klenina)
tel. +38 098 051-92-98
fax. +38 0322 75-77-34